RESEARCH ARTICLE

AMERICAN JOURNAL OF medical genetics

Overgrowth Syndrome Associated With a Gain-of-Function Mutation of the Natriuretic Peptide Receptor 2 (*NPR2*) Gene

Kohji Miura,[1] Ok-Hwa Kim,[2] Hey Ran Lee,[3] Noriyuki Namba,[1] Toshimi Michigami,[4] Won Joon Yoo,[3] In Ho Choi,[3] Keiichi Ozono,[1] and Tae-Joon Cho[3]*

[1]Department of Pediatrics, Osaka University Graduate School of Medicine, Osaka, Japan

[2]Department of Radiology, Ajou University Hospital, Suwon, Republic of Korea

[3]Division of Pediatric Orthopaedics, Seoul National University Children's Hospital, Seoul, Republic of Korea

[4]Department of Bone and Mineral Research, Osaka Medical Centre and Research Institute for Maternal and Child Health, Osaka, Japan

Manuscript Received: 11 March 2013; Manuscript Accepted: 8 August 2013

The signal pathway of the C-type natriuretic (CNP) and its receptor, natriuretic peptide receptor 2 (NPR2) is involved in the longitudinal growth of long bones. Loss of function mutations at NPR2 cause acromesomelic dysplasia, type Maroteaux, while overproduction of CNP by chromosomal translocation and a gain-of-function mutation at NPR2 have been reported to be responsible for an overgrowth syndrome in three cases and one family, respectively. We identified a four-generation family with an overgrowth syndrome characterized by tall stature, macrodactyly of the great toes, scoliosis, coxa valga and slipped capital femoral epiphysis, similar to those previously reported in association with CNP/NPR2 overactivity. The serum level of amino-terminal proCNP was normal in the proband. A novel missense mutation of *NPR2*, c.1462G>C (p.Ala488Pro) was found to co-segregate with the phenotype in this family. In vitro transfection assay of the mutant NPR2 revealed overactivity of the mutant receptor at baseline as well as with the ligand. This overgrowth syndrome caused by a gain-of-function mutation at *NPR2* should be differentiated from Marfan or related syndromes, and may be categorized along with the overgrowth syndrome caused by overproduction of CNP due to its phenotypical similarity as overgrowth CNP/NPR2 signalopathy. © 2013 Wiley Periodicals, Inc.

Key words: tall stature; CNP signal; scoliosis; macrodactyly of the big toe; slipped capital femoral epiphysis

How to Cite this Article:
Miura K, Kim O-H, Lee HR, Namba N, Michigami T, Yoo WJ, Choi IH, Ozono K, Cho T-J. 2014. Overgrowth syndrome associated with a gain-of-function mutation of the natriuretic peptide receptor 2 (NPR2) gene.
Am J Med Genet Part A 164A:156–163.

INTRODUCTION

Natriuretic peptides are a family of hormones/paracrine factors regulating blood volume, blood pressure, ventricular hypertrophy, pulmonary hypertension, fat metabolism, and long bone growth [Potter et al., 2006]. They include atrial natriuretic peptide (ANP; OMIM 600296). CNP binds to a homodimeric transmembrane receptor, natriuretic peptide receptor B/guanylate cylcase B (NPR2; OMIM108961) to increase intracellular level of cyclic guanosine monophosphate (cGMP) [Schulz, 2005]. Several lines of evidence indicate that CNP-NPR2 signaling plays an important role in endochondral ossification [Yasoda et al., 1998; Teixeira et al., 2008]. Inactivation of CNP-NPR2 signaling resulted in dwarfism in both mouse and human. CNP knock-out mice ($Nppc^{-/-}$) or mice with homozygous loss-of-function mutations in *Npr2* result in undergrowth of the skeletal system [Chusho et al., 2001; Tsuji and Kunieda, 2005]. In humans, an autosomal recessive skeletal dysplasia, acromesomelic dysplasia, type Maroteaux (AMDM) characterized by disproportionately mesomelic shortening of the limbs and severe brachydactyly of the hands and feet is caused by homozygous or compound heterozygous loss-of-function mutations in *NPR2* [Bartels et al., 2004]. On the other hand, chronically elevated plasma level of CNP stimulates skeletal

Kohji Miura and Ok-Hwa Kim contributed equally to this work.

Grant sponsor: Ministry for Health, Welfare and Family Affairs Republic of Korea; Grant number: A080588; Grant sponsor: Ministry of Health, Labour and Welfare of Japan; Grant number: KH20Q007a-1.

*Correspondence to:
Tae-Joon Cho, M.D., Division of Pediatric Orthopaedics, Seoul National University Children's Hospital, 101 Daehang-ro Jongno-gu, Seoul 110-744, Republic of Korea.
E-mail: tjcho@snu.ac.kr

Article first published online in Wiley Online Library (wileyonlinelibrary.com): 20 November 2013
DOI 10.1002/ajmg.a.36218

growth in CNP-overproducing transgenic mice [Kake et al., 2009]. In humans, overproduction of CNP due to a chromosomal translocation causes an overgrowth syndrome [Bocciardi et al., 2007; Moncla et al., 2007]. A three-generation Japanese family was recently reported, with an overgrowth syndrome caused by a gain-of-function mutation in *NPR2* [Miura et al., 2012]. We identified and report a four-generation Korean family with similar phenotype and a novel gain-of-function mutation in *NPR2*.

MATERIALS AND METHODS

Clinical Report

This study was approved by the ethics committee at Seoul National University Hospital, and written informed consent was obtained from the proband and family members. An 8-year-old boy visited orthopedic clinic for awkward ambulation and ankle pain on walking. He was a product of normal full term pregnancy with a birth weight 3.2 kg and height 50 cm ($z = -0.04$). His macrodactyly of the big toe was observed since birth, something familiar to his family (Figs. 1 and 2). Developmental milestones were within normal limits. He was recognized as bigger than his age group after the neonatal period. On physical examination at 8 years of age, the height was 145 cm ($z = +3.67$), and weight was 40 kg (>97th centile). He had Marfanoid habitus and arachnodactyly. Neurologic examination was free of abnormal findings. At age 12 years, an unstable slipped capital femoral epiphysis (SCFE) developed on the left hip. Physical examination at this age revealed height 183 cm ($z = +5.19$), weight 71 kg (>97th centile), BMI 21.2 kg/m^2. He showed long and slender fingers and toes, the hallux being remarkably longer than the other toes, ankle valgus deformity, and scoliosis. No anomalies of cardiac valves or the aorta were found on echocardiogram. Blood pressure was within normal limits. No abnormality was observed in ophthalmic and otologic examinations. Hematological, biochemical and endocrinological values including insulin-like growth factor-I (IGF-I) were within normal ranges. However, bone formation and resorption markers were increased—osteocalcin, 118 ng/ml (reference range, 8–50); urinary cross-linked N-telopeptide of type I collagen, 969 BCE/mM creatinine (reference range, 21–83). Bone mineral density of L2-4 as measure by dual energy X-ray absorptiometry (Lunar Prodigy Advance, GE Healthcare, Waukesha, WI) was 0.791g/cm^2 ($z = -0.3$). Considering the tall stature of this patient, this BMD result may suggest presence of more severe osteopenia. Radiological survey of the skeleton showed coxa valga deformity of the femora, slipped capital femoral epiphysis, and lumbar scoliosis (Fig. 3). Arachnodactyly of all fingers and toes; of these, disproportionately long and large great toes were observed. Investigation of the family history revealed a four-generation family with 11 family members including the proband that could be considered to have the same phenotype. Five of 11 affected members were examined. They were characterized by tall stature (exceeded +4 SD compared to age matched control height of Korean population) and markedly long big toes. All of them showed coxa valga deformity with epiphyseal dysplasia of the femoral capital epiphyses and two had SCFE (Fig. 4). Three of them had lumbar scoliosis. The vertebral bodies were tall and showing endplate irregularities and narrowing of the intervertebral disc spaces in four of them. As seen in the clinical phenotype, radiograph of the feet showed extremely elongated metatarsals and assorted phalanges of the great toe symmetrically. The hands of all affected individuals showed arachnodactyly without elongation of specific fingers.

Mutation Analysis

Genomic DNA was extracted from the circulating leukocytes from the proband and family members available (Fig. 1). All the exons of *CNP*, *NPR2*, Natriuretic peptide receptor C (*NPR3*; MIM108962), and fibroblast growth factor receptor 3 (*FGFR3*; MIM134934) were

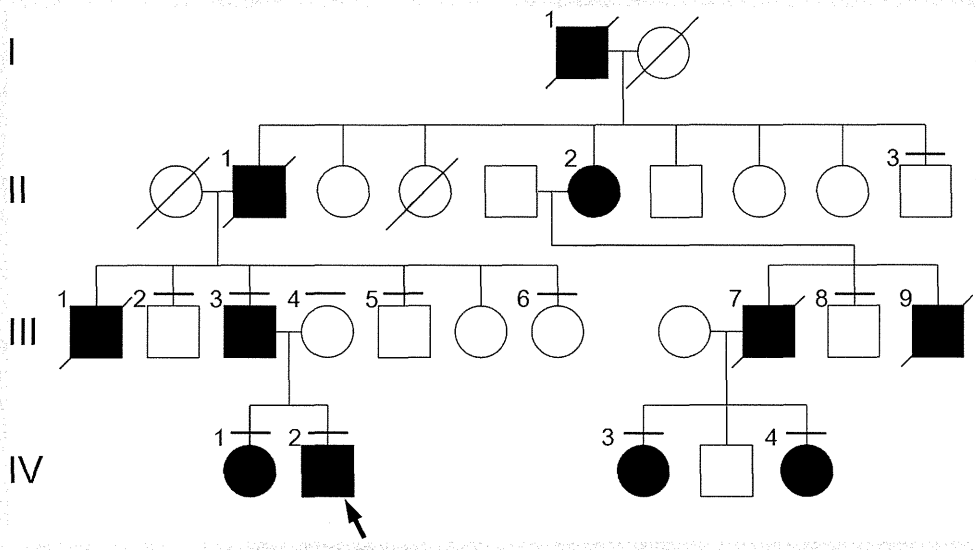

FIG. 1. Pedigree of the family. There are several father-to-son transmissions of the phenotype, revealing autosomal dominant inheritance pattern. Transverse bars above the circles or rectangles denote those who underwent mutation study. An arrow indicates the proband.

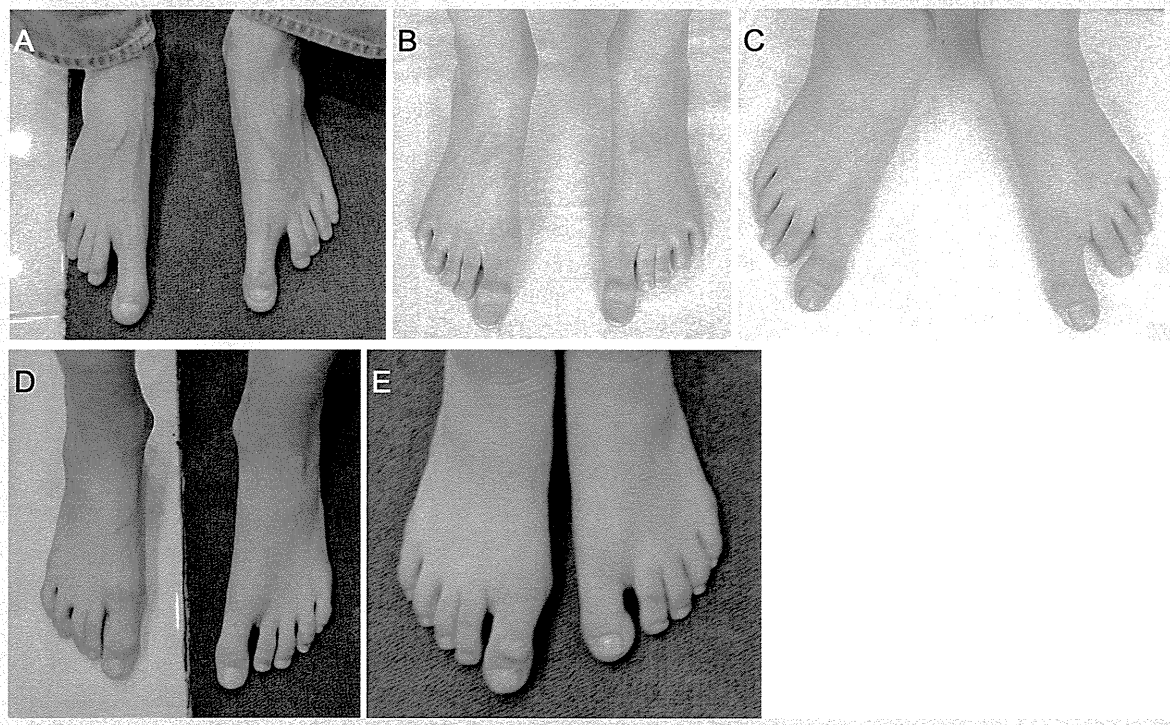

FIG. 2. Photographs of the feet of the affected family members. A: III-3, (B) IV-1, (C) IV-2, (D) IV-3, (E) IV-4. Patients IV-3 and IV-4 show relatively mild macrodactyly of the big toes as compared with the others.

amplified using specific primers [Miura et al., 2012] flanking the intron–exon boundaries according to published human genomic DNA sequences (UCSC genome browser: uc002vsl.1 at chromosome 2, 232498379–232499203; uc003zyd.1 at chromosome 9, 35782406–35799728; uc003jhv.2 at chromosome 5, 32711665–32787252; uc003gds.2 at chromosome 4, 1764337–1780396, respectively). Polymerase chain reaction (PCR) products was sequenced using a Big Dye terminator cycle sequencing kit (version 3.1; Applied Biosystems, Foster City, CA) and an ABI 3130 automated sequencer (Applied Biosystems).

Measurement of Serum Amino-Terminal (NT) proCNP Concentrations

Serum of IV-2 and III-3 were separated and collected, and NT-proCNP was assayed using an enzyme immunoassay (BIOMEDICA, Vienna, Austria) according to the instructions provided. As a control, samples from eight healthy Japanese teenager boys and five women were also measured.

In Vitro Transfection Assay of Mutant NPR2

The pcDNA3.1(+)/hemagglutinin (HA)-tagged human NPR2 wild-type vector (HA-WT) was a gift from Dr. Yoshihiro Ogawa (Tokyo Medical and Dental University, Japan) [Hachiya et al., 2007]. The construct encoding the mutant p.Ala488Pro, pcDNA3.1(+)/HA-human NPR-2 Ala488Pro (HA-Ala488Pro), was generated by PCR-based mutagenesis using HA-WT as the template, and primers containing the nucleotide change. All vector constructs were verified by bidirectional DNA sequencing.

HEK293A cells at confluence were transfected with empty vector containing green fluorescent protein(GFP), HA-WT, and HA-Ala488Pro using the liposomal transfection reagent FuGENE6 (Reagent: DNA = 3 μl: 0.5 μg, Roche, Indianapolis, IN, 12-well plate), according to the manufacturer's instructions. In 48 hr, cell lysate was harvested and immunoblot was performed to compare the expression of transfected genes, using a mouse monoclonal antibody against HA-tag (6E2, 1:1,000; Cell Signaling Technology, Boston, MA) as the primary antibody. As an internal control, β-actin in each sample was detected with a monoclonal anti-β-actin antibody (1:5,000; SIGMA-ALDRICH, Saint Louis, MO).

Transfected cells were serum-starved for 24 hr before the cGMP assay and then incubated at 37°C with 5% CO_2 in DMEM containing 0.5 mM IBMX (3-isobutyl-1-methylxanthine) (Wako, Osaka, Japan) for 10 min. The cells were next treated with vehicle (water) or 1×10^{-7} M CNP-22 (Biochem Life Sciences, New Delhi, India) and incubated for another 10 min. The reaction was terminated with 300 μl of 0.1 M HCl, and the cGMP concentration was measured by a competitive enzyme immunoassay (Cayman Chemical, Ann Arbor, MI). Results are presented as the mean ± SD. Student's *t* test was used for statistical analyses.

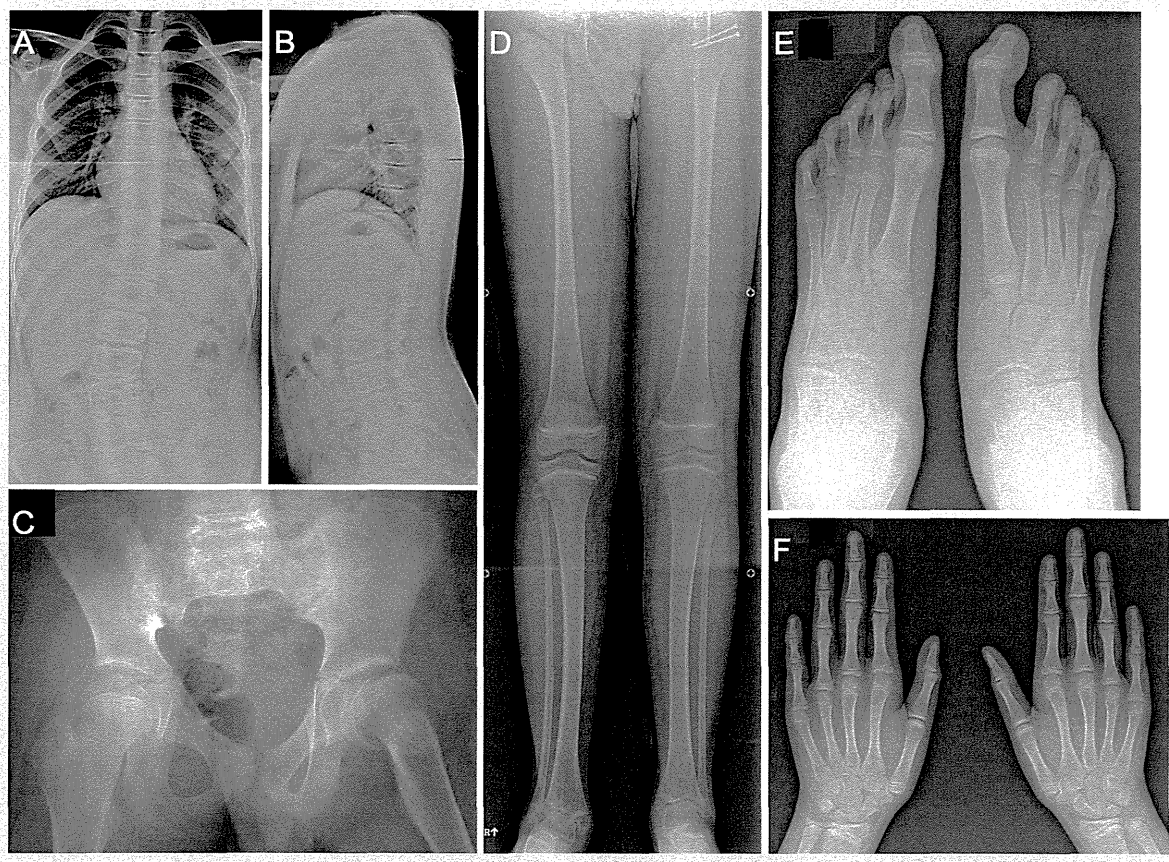

FIG. 3. Skeletal survey of the proband at age 12 years. A,B: Anteroposterior and lateral spine show lumbar scoliosis, slightly tall vertebral bodies with irregular end-plates, and narrowing of the intervertebral disc spaces. C: Pelvis shows coxa valga deformity and slipped femoral capital epiphysis on the left hip. D: Lower extremity demonstrates long and slender long bones with thin cortices. Mild inward bowing of the tibial and fibular diaphysis and ankle valgus deformity are noted. E: Feet show exceedingly long and large metatarsals and phalanges of the great toes symmetrically. F: Hands show overall arachnodactyly without specific digit elongation. Carpal bone age is advanced, measuring approximately 14 years of age.

RESULTS

Identification of a Novel Missense Mutation p.Ala488Pro in *NPR2*

On screening the sequences of exons of *CNP*, *NPR2*, *NPR3*, and *FGFR3* in the proband and family members as depicted on Figure 1, we identified a novel heterozygous sequence variation c. 1462G>C at *NPR2* in those who shared the similar phenotype (III-3, IV-1, IV-2, IV-3, and IV-4), but not in the remaining unaffected family members. The sequence variation eliminates an *Nhe*I cleavage site. PCR product of wild type containing this site (484 bp) would be cut into 95 and 389 bp fragments. Hence, these PCR products from all the patients tested were incubated with *Nhe*I (New England BioLabs, Ipswiich, MA) overnight and run on an agarose gel to confirm the presence of this sequence variation. It showed that this sequence variation perfectly co-segregated with the phenotype in this family. It was predicted to substitute alanine for proline (p. Ala488Pro). This variant was not registered in the dbSNP (build 137) (http://www.ncbi.nlm.nih.gov/projects/SNP/) nor in the NHLBI Exome Sequencing Project (ESP) (http://evs.gs.washington.edu/EVS/). It was not found in 400 alleles from healthy Korean or Japanese controls, either. Amino acid Ala488 is located in a highly conserved region of the juxtamembranous cytoplasmic domain of NPR2 and is conserved across species (Fig. 5). No mutations were found in *CNP*, *NPR3*, or *FGFR3*.

CNP Was Not Overproduced in the Proband

Serum NT-proCNP levels of the proband (IV-2) and his mother were measured 9.68 and 2.65 pmol/L, respectively. Those of eight Japanese teenager boys of age ranging from 12 to 14 years averaged 6.0 ± 3.4 pmol/L (mean $\pm$ standard deviation), and of five Japanese female adults of age ranging from 32 to 48 averaged 4.0 ± 0.9 pmol/L (unpublished data).

p.Ala488Pro Is a Gain-of-Function Mutation

To investigate the pathogenic significance of the p.Ala488Pro mutation, an in vitro functional assay was performed. HEK293A

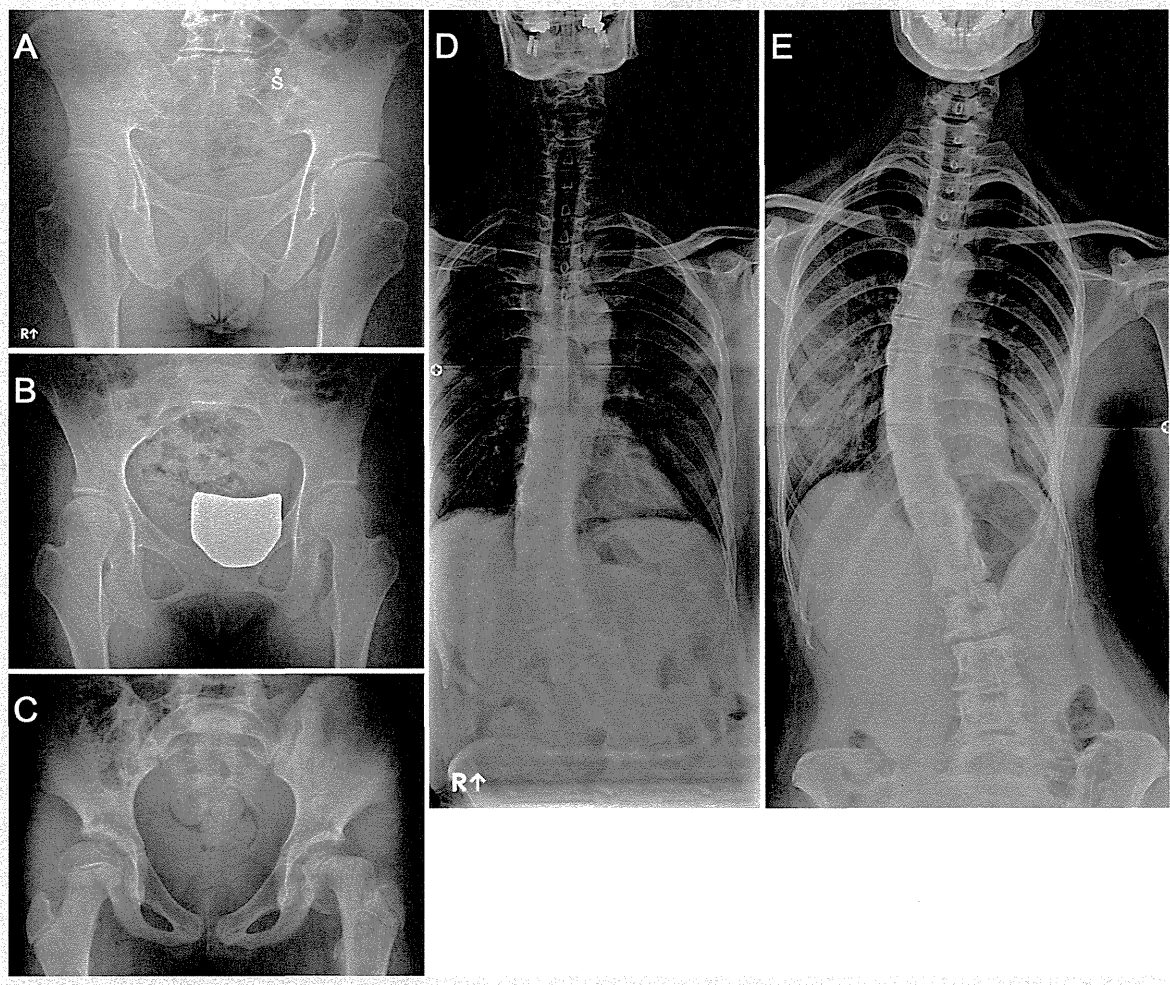

FIG. 4. Radiographs of the pelvis and spine of the other affected family members. Marked coxa valga deformity and residual valgus slipped capital femoral epiphysis are seen in Patients III-3 (A) and IV-1 (B). C: Coxa valga deformity and unstable aggravation of the slipped capital femoral epiphysis at the left hip are seen in Patient IV-3 at age 11 years. D: Patient III-3 and (E) Patient IV-1 show thoracolumbar scoliosis. The vertebral bodies are tall and narrowing of the disc spaces is noted.

cells were transfected with the GFP, HA-WT, and HA-Ala488Pro. The Western blot analysis using anti-HA antibody confirmed that HA-WT and HA-Ala488Pro were expressed at comparable levels, with an approximate molecular size of 120 kDa (Fig. 6A). cGMP production in the cells expressing HA-WT, and HA-Ala488Pro was also examined. cGMP was produced in Ala488Pro-expressing cells, even in the absence of CNP, while no production was observed in HA-WT-expressing cells. Treatment with CNP-22 at a dose of 1×10^{-7} M increased intracellular cGMP levels with concentrations significantly higher in HA-Ala488Pro than in HA-WT-expressing cells (Fig. 6B). These results indicate that p.Ala488Pro is a gain-of-function type mutation.

DISCUSSION

The CNP/NPR2 signal pathway is involved in the longitudinal growth of skeletal system [Yasoda et al., 1998; Chusho et al., 2001; Bartels et al., 2004; Tsuji and Kunieda, 2005; Bocciardi et al., 2007; Moncla et al., 2007; Teixeira et al., 2008; Kake et al., 2009]. Miura et al. [2012] reported a Japanese family with an overgrowth syndrome caused by a gain-of-function mutation at *NPR2*. The current study reports a second family showing a similar phenotype inherited as an autosomal dominant trait. The affected family members harbor a novel gain-of-function mutation at *NPR2*, c.1462G>C (p.Ala488Pro).

The mutation of the current family is located at a topological domain between transmembrane and protein kinase domainsrot[UniProtKB[Internet]], while the previously reported gain-of-function mutation was at the guanylate cyclase domain [Miura et al., 2012]. Although the current mutation does not exist at the guanylate cyclase domain, it must bring conformational change at the 3D structure of guanylate cyclase domain to enhance its enzymatic activity with or without binding the ligand.

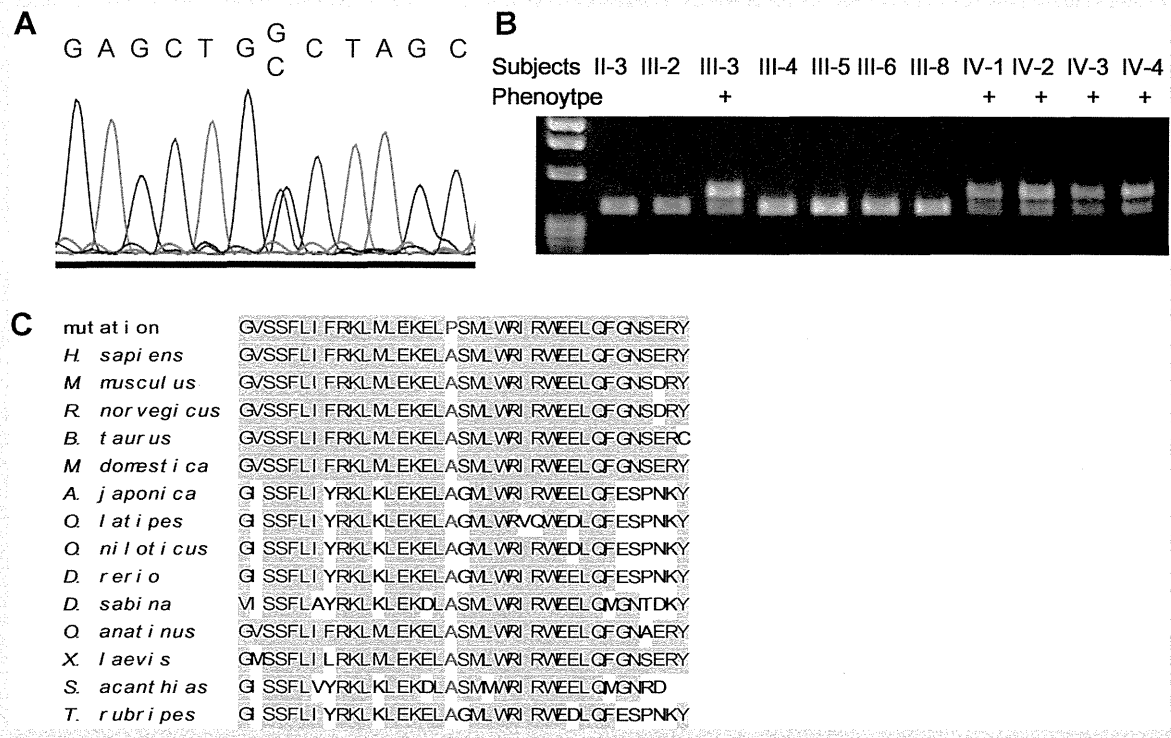

FIG. 5. Identification of the *Npr2* mutation. Sanger sequencing of the *NPR2* revealed a novel G → C missense mutation at nucleotide +1,462 creates a substitution, proline for alanine, at codon 488 in a heterozygous state. Among the subjects tested, this mutation was present in all the patients having the phenotype, and absent in all those who did not (A). This mutation eliminated the cleavage site of *Nhe*I, producing two bands on gel electrophoresis when treated with *Nhe*I (B). Amino acid alignment of NPR2 among various species. Alanine at codon 488 is located in a highly conserved cytoplasmic region between the transmembrane and protein kinase domains of NPR2 (C).

NPR2 is an interesting example of phenotypes contrasting between gain-of-function versus loss-of-function mutations at a gene encoding a receptor protein. Homozygous or compound heterozygous loss-of-function mutations of *NPR2* in humans cause a specific skeletal dysplasia, AMDM, characterized by marked short stature as well as short fingers and toes. The overgrowth syndrome by gain-of-function mutation seems to have phenotype opposite to that of AMDM. It is also interesting to note that the increased NPR2 activity did not suppress CNP production, maintaining its serum level within normal limit. The same unsuppressed CNP production was also observed in the previous cases of gain-of-function mutation at *NPR2* [Miura et al., 2012], suggesting lack of feedback loop between the NPR2 activity and CNP production.

This family has noticed 11 affected members by tall stature and long big toes through four generations. Neither macrodactyly of the big toe and ankle valgus deformity nor scoliosis and residual proximal femoral deformity of SCFE interferes with their daily living activities. One of them (IV-3) had even played basketball in a high school varsity team. However, development of unstable SCFE threatened function of the hip joint, and the proband was required to have major hip surgeries. SCFE is a chronic, gradual displacement of the femoral head at the proximal femoral physis. It may remain silent until physeal closure, and end up with residual deformity at the proximal femur as in the Patients III-3 and IV-1 (Fig. 4). However, in some cases, the SCFE could aggravate suddenly, resulting in unstable separation of the femoral head as in Patients IV-2 and IV-4 (Figs. 3 and 4), which is an orthopedic emergency requiring surgical intervention to stabilize the femoral head and to preserve its viability. Hence, once this disease entity is recognized, the patient should have an orthopedic consultation to monitor development and progress of SCFE, which was exclusively harbored by the affected members in this family. It is noteworthy that a residual deformity of silent SCFE showed posterolateral displacement of the femoral head (Fig. 4), a rare subtype of SCFE [Loder et al., 2006]. Scoliosis did not require any intervention in these affected family members. Macrodactyly of the big toes were not complained of in shoe fitting or cosmesis in the proband and affected family members.

The characteristic clinical and radiological findings make it a specific, discernible clinical disease entity, which can be differentiated from Marfan or other related syndromes. However, it is very similar to a phenotype caused by chromosomal translocation of 2q37 and subsequent CNP overproduction [Bocciardi et al., 2007; Moncla et al., 2007]. Hence, CNP overproduction and its receptor gene gain-of-function mutation may be categorized into a disease entity, that is, overgrowth CNP/NPR2 signalopathy, which should be included in differential diagnosis of the overgrowth syndrome.

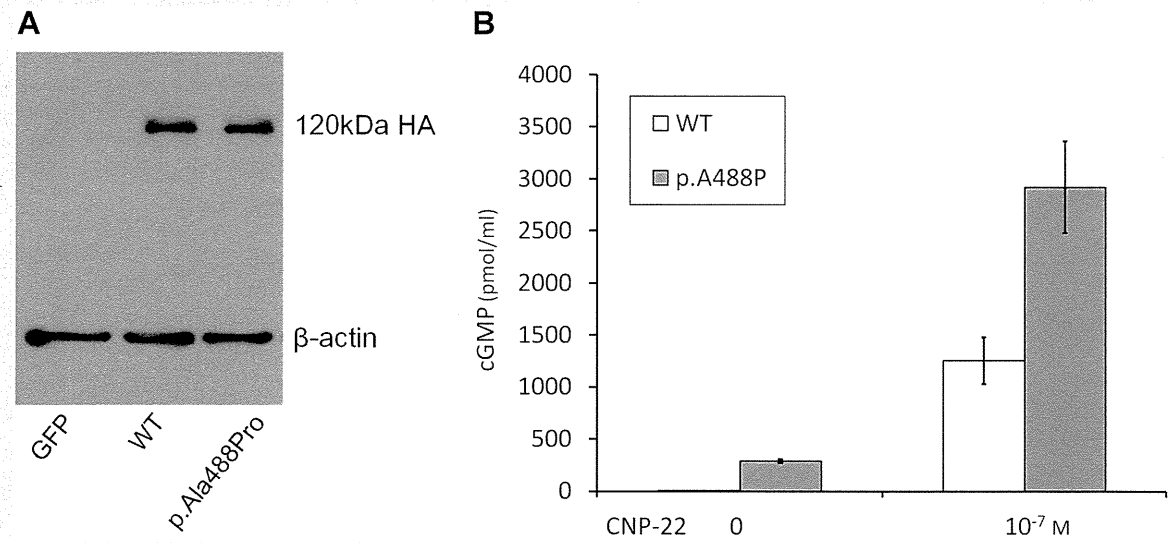

FIG. 6. NPR2 mutation of p.Ala488Pro is a gain-of-function mutation. A: Western blot analysis confirmed the comparable expression of HA-WT (WT) and HA-Ala488Pro. As an internal control, β-actin in each sample was detected with anti-β-actin antibody. B: Increased cGMP production in the HEK293A cells transfected with the p.Ala488Pro mutant compared to that in wild-type cells (WT). Forty-eight hours after the transfection, the cells were serum-starved for 24 hr, and then treated with the indicated concentrations of CNP-22 for 10 min, before cGMP production was assayed. Results are presented as the mean ± SD (N = 3, *$P < 0.05$).

In summary, we report on a family with an overgrowth syndrome inherited as autosomal dominant trait, which is caused by a gain-of-function mutation at *NPR2*. This is a distinct clinical entity that can be differentiated from other overgrowth syndromes by its clinical and radiological manifestations. Recognition of this specific disease entity will lead to targeted molecular study for confirmation, and will alert the clinician for potentially serious complication such as unstable SCFE.

ACKNOWLEDGMENTS

This study was supported in part by a grant from Ministry for Health, Welfare and Family Affairs, Republic of Korea (A080588) and in part by Grants-in-aid from the Ministry of Health, Labour and Welfare of Japan (KH20Q007a-1).

REFERENCES

Bartels CF, Bukulmez H, Padayatti P, Rhee DK, van Ravenswaaij-Arts C, Pauli RM, Mundlos S, Chitayat D, Shih LY, Al-Gazali LI, Kant S, Cole T, Morton J, Cormier-Daire V, Faivre L, Lees M, Kirk J, Mortier GR, Leroy J, Zabel B, Kim CA, Crow Y, Braverman NE, van den Akker F, Warman ML. 2004. Mutations in the transmembrane natriuretic peptide receptor NPR-B impair skeletal growth and cause acromesomelic dysplasia, type Maroteaux. Am J Hum Genet 75:27–34.

Bocciardi R, Giorda R, Buttgereit J, Gimelli S, Divizia MT, Beri S, Garofalo S, Tavella S, Lerone M, Zuffardi O, Bader M, Ravazzolo R, Gimelli G. 2007. Overexpression of the C-type natriuretic peptide (CNP) is associated with overgrowth and bone anomalies in an individual with balanced t(2;7) translocation. Hum Mutat 28:724–731.

Chusho H, Tamura N, Ogawa Y, Yasoda A, Suda M, Miyazawa T, Nakamura K, Nakao K, Kurihara T, Komatsu Y, Itoh H, Tanaka K, Saito Y, Katsuki M. 2001. Dwarfism and early death in mice lacking C-type natriuretic peptide. Proc Natl Acad Sci USA 98:4016–4021.

Hachiya R, Ohashi Y, Kamei Y, Suganami T, Mochizuki H, Mitsui N, Saitoh M, Sakuragi M, Nishimura G, Ohashi H, Hasegawa T, Ogawa Y. 2007. Intact kinase homology domain of natriuretic peptide receptor-B is essential for skeletal development. J Clin Endocrinol Metab 92:4009–4014.

Kake T, Kitamura H, Adachi Y, Yoshioka T, Watanabe T, Matsushita H, Fujii T, Kondo E, Tachibe T, Kawase Y, Jishage K, Yasoda A, Mukoyama M, Nakao K. 2009. Chronically elevated plasma C-type natriuretic peptide level stimulates skeletal growth in transgenic mice. Am J Physiol Endocrinol Metab 297:E1339–E1348.

Loder RT, O'Donnell PW, Didelot WP, Kayes KJ. 2006. Valgus slipped capital femoral epiphysis. J Pediatr Orthop 26:594–600.

Miura K, Namba N, Fujiwara M, Ohata Y, Ishida H, Kitaoka T, Kubota T, Hirai H, Higuchi C, Tsumaki N, Yoshikawa H, Sakai N, Michigami T, Ozono K. 2012. An overgrowth disorder associated with excessive production of cGMP due to a gain-of-function mutation of the natriuretic peptide receptor 2 gene. PLoS ONE 7:e42180.

Moncla A, Missirian C, Cacciagli P, Balzamo E, Legeai-Mallet L, Jouve JL, Chabrol B, Le Merrer M, Plessis G, Villard L, Philip N. 2007. A cluster of translocation breakpoints in 2q37 is associated with overexpression of NPPC in patients with a similar overgrowth phenotype. Hum Mutat 28:1183–1188.

Potter LR, Abbey-Hosch S, Dickey DM. 2006. Natriuretic peptides, their receptors, and cyclic guanosine monophosphate-dependent signaling functions. Endocr Rev 27:47–72.

Schulz S. 2005. C-type natriuretic peptide and guanylyl cyclase B receptor. Peptides 26:1024–1034.

Teixeira CC, Agoston H, Beier F. 2008. Nitric oxide, C-type natriuretic peptide and cGMP as regulators of endochondral ossification. Dev Biol 319:171–178.

Tsuji T, Kunieda T. 2005. A loss-of-function mutation in natriuretic peptide receptor 2 (Npr2) gene is responsible for disproportionate dwarfism in cn/cn mouse. J Biol Chem 280:14288–14292.

UniProtKB[Internet]. UniProt Consortium (EMBL-EBI, PIR, and SIB) [2002]. P20594(ANPRB_HUMAN) [updated January 9, 2013 Version 151, Cited January 12, 2013]. Available from http://www.uniprot.org/uniprot/P20594

Yasoda A, Ogawa Y, Suda M, Tamura N, Mori K, Sakuma Y, Chusho H, Shiota K, Tanaka K, Nakao K. 1998. Natriuretic peptide regulation of endochondral ossification. Evidence for possible roles of the C-type natriuretic peptide/guanylyl cyclase-B pathway. J Biol Chem 273: 11695–11700.

Pediatr Radiol
DOI 10.1007/s00247-014-3013-1

CASE REPORT

A case of severe proximal focal femoral deficiency with overlapping phenotypes of Al-Awadi-Raas-Rothschild syndrome and Fuhrmann syndrome

Masaki Matsushita · Hiroshi Kitoh · Kenichi Mishima · Yoshihiro Nishida · Naoki Ishiguro

Received: 6 January 2014 / Revised: 2 April 2014 / Accepted: 23 April 2014

Abstract Proximal focal femoral deficiency (PFFD) is a heterogeneous disorder characterized by various degrees of femoral deficiencies and associated anomalies of the pelvis and lower limbs. The etiology of the disease has not been determined. We report on a 3-year-old boy with severe PFFD, who showed almost completely absent femora and fibulae, malformed pelvis and ectrodactyly of the left foot. These features were partially overlapped with those of Al-Awadi-Raas-Rothschild syndrome or Fuhrmann syndrome, both of which are caused by *WNT7A* mutations. Molecular analysis of our case, however, demonstrated no disease-causing mutations in the *WNT7A* gene.

Keywords Proximal focal femoral deficiency · Al-Awadi-Raas-Rothschild syndrome · Fuhrmann syndrome · WNT7A · Molecular analysis · Radiography · Child

Introduction

Proximal focal femoral deficiency (PFFD) is a rare congenital anomaly of the pelvis and proximal femur with several degrees of shortening of the involved lower limb. The condition may be unilateral or bilateral and is often associated with other congenital anomalies. The cause of PFFD is uncertain, but several etiological factors have been suggested, including poor diabetic control, exposure to drugs (thalidomide), viral infections, radiation, focal ischemia and trauma between the 4th and 8th weeks of gestation [1]. The Aitken classification is the most widely used system for classifying PFFD based on the radiographic appearance ranking from a benign form (Type A) to a severe form (Type D) according to the extent of femoral deficiency [2]. In Type D, the femoral head and acetabulum are absent, and the shaft of the femur is extremely short or absent. There is a phenotypic similarity between the cases with Type D PFFD and those with Al-Awadi-Raas-Rothschild syndrome or Fuhrmann syndrome. These two syndromes have recently been reported to be associated with the *WNT7A* mutations. Both syndromes share similar clinical features, but the phenotype in Fuhrmann syndrome is less severe [3].

Here, we report on a 3-year-old boy who showed severe malformations of the pelvis and bilateral lower limbs without associated severe upper limbs anomalies. The findings of our case were similar to those of Fuhrmann syndrome rather than those of Al-Awadi-Raas-Rothschild syndrome. Molecular analyses, however, demonstrated negative for the *WNT7A* mutations in the present case.

Case report

The proband, a Japanese boy, was the first child born to healthy, nonconsanguineous parents. His mother did not suffer from diabetes mellitus. His younger brother was normal. Family history of skeletal dysplasia was negative. Bilateral femoral deficiencies were found at his second trimester. He was delivered at 36 weeks of gestation with a birth weight of 1,884 g (−1.8 SD for gestational age) and a height of 36 cm (−4.2 SD for gestational age) by Cesarean section. The Apgar score was 6 at 1 min.

He was referred to us at age 12 days for severe malformations of bilateral lower limbs. On physical examinations, bilateral thighs were extremely short so that the lower

M. Matsushita · H. Kitoh (✉) · K. Mishima · Y. Nishida · N. Ishiguro
Department of Orthopaedic Surgery,
Nagoya University Graduate School of Medicine,
65 Tsurumai, Showa-ku, Nagoya, Aichi 466-8550, Japan
e-mail: hkitoh@med.nagoya-u.ac.jp

Published online: 18 May 2014

legs seemed to be connected with the pelvis. There was a varus deformity in the right foot associated with syndactyly of the third and fourth toes and a valgus deformity in the left foot (Fig. 1). He showed flexion contracture of the proximal interphalangeal joint in his left middle and ring fingers. Facial appearance seemed to be normal. Radiographic examinations at the age of 4 months revealed hypoplastic ilia, absent acetabula, and malformed pubic and ischial bones. The left femur was absent, while there was a rudimentary distal femur in the right. Bilateral fibulae were also absent. Bilateral tibiae were slender and there was a large round epiphysis in the left proximal tibia (Fig. 2). The tarsal bones were unremarkable but an ectrodactyly of the left foot was observed (Fig. 2). The spine, thorax and upper limbs were unremarkable. Chromosomal analysis was also normal.

Extraskeletal abnormalities included a left inguinal hernia that was surgically treated at the age of 2 months and an abdominal pressure-induced incontinence with no association of hydronephrosis and ureteral dilatation. Magnetic resonance imaging (MRI) of the whole spine showed no abnormalities. His cognitive development was normal. Varus deformity of his right foot was treated with serial casting and subsequent bracing, while his left valgus foot was spontaneously corrected. Flexion contracture of his left fingers was healed by an application of splinting. He could walk with two Lofstrand crutches at 3 years old. He was diagnosed to have PFFD Type D but his clinical and radiographic features were partially overlapped with those of Al-Awadi-Raas-Rothschild syndrome or Fuhrmann syndrome (Table 1).

After informed consent was obtained from his family, genomic DNA from peripheral blood of the proband was extracted using the QIAampDNABlood Midi kit (Qiagen Inc., Valencia, CA). Direct sequencing of the complete coding regions and exon-intron boundaries of the *WNT7A* gene was performed using the CEQ 8000 Sequencer (Beckman Coulter, Fullerton, CA) according to the manufacturer's instructions. The primers used for amplification and sequencing of the

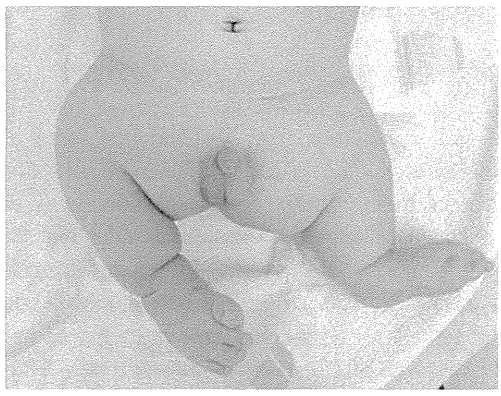

Fig. 1 A clinical photo of the lower limbs and trunk at the age of 5 months. Marked shortening of bilateral lower limbs, varus foot with syndactyly of the third and fourth toes in the right, and valgus foot in the left are demonstrated

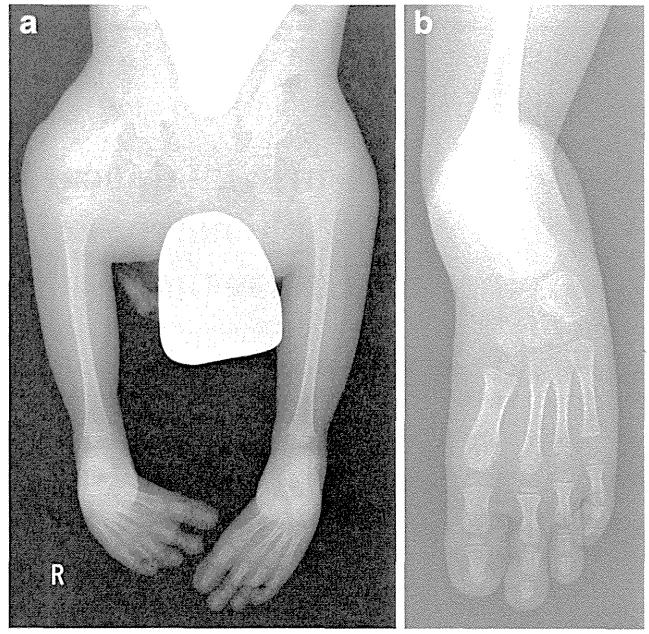

Fig. 2 Anteroposterior radiographs at the age of 3.5 years. **a** The pelvis and lower limbs demonstrate small and narrow ilia, malformed ischiopubic bones, deficient acetabula, complete absent of the left femur, rudimentary right femur, absent fibulae and slender tibiae with ball-shaped large epiphysis of the left tibia. **b** The left foot demonstrates four pairs of metatarsals and phalanges without deformity of tarsal bones

WNT7A gene were described previously [4]. Two reported heterozygous variants, c.315G>A and c.459 T>C in exon 3 of the *WNT7A*, both of which are known synonymous single-nucleotide polymorphisms (SNPs), were found in the proband.

Table 1 Comparison of phenotypes among Al-Awadi-Raas-Rothschild syndrome and Fuhrmann syndrome and present case

Al-Awadi-Raas-Rothschild syndrome and Fuhrmann syndrome		Present case
Facial dysmorphism	±	−
Thorax anomaly	±	−
Upper limp anomaly	+	±
Urinary tract anomaly	±	±
Pelvis dysplasia	+	+
Lower limbs		
Aplastic/hypoplastic femur	+	+
Aplastic/hypoplastic fibula	+	+
Aplastic/hypoplastic tibia	+	−
Bilateral involvement	+	+
Stick-like appendage	+	−
Feet		
Ectrodactyly	+	+
Hypoplastic nails	+	−

+positive, ± occasionally positive or suspected, − negative

Discussion

Congenital femoral deficiencies can be seen in a variety of diseases including PFFD, femoral hypoplasia-unusual facies syndrome [5], femur-fibula-ulna syndrome [6], Al-Awadi-Raas-Rothschild syndrome and Fuhrmann syndrome [7]. The absence of craniofacial anomalies and upper limb malformations distinguishes our case from femoral hypoplasia-unusual facies syndrome and femur-fibula-ulna syndrome. Al-Awadi-Raas-Rothschild syndrome and Fuhrmann syndrome, both of which are known to be associated with the *WNT7A* mutations, have similar clinical features including limb and pelvic deficiencies and abnormal genitalia. Generally, more severe defects of the upper limbs are seen in Al-Awadi-Raas-Rothschild syndrome than in Fuhmann syndrome. There is complete and partial loss of *WNT7A* function in these two syndromes, respectively [3]. *WNT7A* molecules regulate the dorsal-ventral and anterior-posterior axes and outgrowth of limbs. The anterior-posterior axis determines the development of fibulo-tibial structures in the foot/leg. Absent femora and fibulae, ectrodactyly of the foot and pelvic dysplasia found in the present case seemed to result from the impairment of anterior-posterior patterning and outgrowth of limbs. Our case, however, only showed minimal upper limb abnormalities (mild contracture of fingers) and lacked the phenotypes of dorsal-ventral axis deficiency such as hypoplastic nails. Negative *WNT7A* mutations could differentiate our PFFD case from Al-Awadi-Raas-Rothschild syndrome or Fuhrmann syndrome, although minor deletions or duplications within the *WNT7A* gene could not be ruled out in the present study.

Kantaputra and Tanpaiboon [8] reported on a 3-year-old Thai boy with severe malformations of the upper and lower limbs, pelvis and genital organs. The majority of findings overlapped with those of Al-Awadi-Raas-Rothschild syndrome, but the presence of humeroulnar synostosis and predominant radial ray abnormalities and absence of nail dysplasia were different features from typical cases of Al-Awadi-Raas-Rothschild syndrome [8]. Except the upper limb deficiencies, their case had similar phenotypes to our case including hypoplastic ilium, poorly formed acetabula, absent femora and fibulae, slender tibiae with malformed proximal epiphysis and normal facial appearance. These cases may be included in the entity of diseases in the limb-pelvis developmental field.

In conclusion, we present a case of severe PFFD with some overlapping phenotypes of Al-Awadi-Raas-Rothschild syndrome and Fuhrmann syndrome without associated *WNT7A* mutation. Further molecular studies will be needed to determine the basic defects of our case.

Conflicts of interest None.

References

1. Epps CH Jr (1983) Proximal femoral focal deficiency. J Bone Joint Surg Am 65:867–870
2. Aitken GT (1969) In: Aitken GT (ed) Proximal femoral focal deficiency: definition, classification, and management. National Academy of Sciences, Washington, pp 1–22
3. Woods CG, Stricker S, Seemann P et al (2006) Mutations in WNT7A cause a range of limb malformations, including Fuhrmann syndrome and Al-Awadi/Raas-Rothschild/Schinzel phocomelia syndrome. Am J Hum Genet 79:402–408
4. Shyy W, Dietz F, Dobbs MB et al (2009) Evaluation of CAND2 and WNT7a as candidate genes for congenital idiopathic clubfoot. Clin Orthop Relat Res 467:1201–1205
5. Daentl DL, Smith DW, Scott CI et al (1975) Femoral hypoplasia-unusual facies syndrome. J Pediatr 86:107–111
6. Lenz W, Zygulska M, Horst J (1993) FFU complex: an analysis of 491 cases. Hum Genet 91:347–356
7. AlQattan MM, AlAbdulkareem I, Ballow M et al (2013) A report of two cases of Al-Awadi Raas-Rothschild syndrome (AARRS) supporting that "apparent" Phocomelia differentiates AARRS from Schinzel Phocomelia syndrome (SPS). Gene 527:371–375
8. Kantaputra PN, Tanpaiboon P (2005) A newly recognized syndrome involving limbs, pelvis, and genital organs or a variant of Al-Awadi/Raas-Rothschild syndrome? Am J Med Genet A 132:63–67

ORPHANET JOURNAL OF RARE DISEASES

RESEARCH Open Access

Japanese founder duplications/triplications involving *BHLHA9* are associated with split-hand/foot malformation with or without long bone deficiency and Gollop-Wolfgang complex

Eiko Nagata[1†], Hiroki Kano[2†], Fumiko Kato[1], Rie Yamaguchi[1], Shinichi Nakashima[1], Shinichiro Takayama[3], Rika Kosaki[4], Hidefumi Tonoki[5], Seiji Mizuno[6], Satoshi Watanabe[7], Koh-ichiro Yoshiura[7], Tomoki Kosho[8], Tomonobu Hasegawa[9], Mamori Kimizuka[10], Atsushi Suzuki[11], Kenji Shimizu[11], Hirofumi Ohashi[11], Nobuhiko Haga[12], Hironao Numabe[13], Emiko Horii[14], Toshiro Nagai[15], Hiroshi Yoshihashi[16], Gen Nishimura[17], Tatsushi Toda[18], Shuji Takada[19], Shigetoshi Yokoyama[19,22], Hiroshi Asahara[19,20], Shinichiro Sano[1,21], Maki Fukami[21], Shiro Ikegawa[2] and Tsutomu Ogata[1*]

Abstract

Background: Limb malformations are rare disorders with high genetic heterogeneity. Although multiple genes/loci have been identified in limb malformations, underlying genetic factors still remain to be determined in most patients.

Methods: This study consisted of 51 Japanese families with split-hand/foot malformation (SHFM), SHFM with long bone deficiency (SHFLD) usually affecting the tibia, or Gollop-Wolfgang complex (GWC) characterized by SHFM and femoral bifurcation. Genetic studies included genomewide array comparative genomic hybridization and exome sequencing, together with standard molecular analyses.

Results: We identified duplications/triplications of a 210,050 bp segment containing *BHLHA9* in 29 SHFM patients, 11 SHFLD patients, two GWC patients, and 22 clinically normal relatives from 27 of the 51 families examined, as well as in 2 of 1,000 Japanese controls. Families with SHFLD- and/or GWC-positive patients were more frequent in triplications than in duplications. The fusion point was identical in all the duplications/triplications and was associated with a 4 bp microhomology. There was no sequence homology around the two breakpoints, whereas rearrangement-associated motifs were abundant around one breakpoint. The rs3951819-*D17S1174* haplotype patterns were variable on the duplicated/triplicated segments. No discernible genetic alteration specific to patients was detected within or around *BHLHA9*, in the known causative SHFM genes, or in the exome.

(Continued on next page)

* Correspondence: tomogata@hama-med.ac.jp
†Equal contributors
[1]Department of Pediatrics, Hamamatsu University School of Medicine, Hamamatsu 431-3192, Japan
Full list of author information is available at the end of the article

(Continued from previous page)

Conclusions: These results indicate that *BHLHA9* overdosage constitutes the most frequent susceptibility factor, with a dosage effect, for a range of limb malformations at least in Japan. Notably, this is the first study revealing the underlying genetic factor for the development of GWC, and demonstrating the presence of triplications involving *BHLHA9*. It is inferred that a Japanese founder duplication was generated through a replication-based mechanism and underwent subsequent triplication and haplotype modification through recombination-based mechanisms, and that the duplications/triplications with various haplotypes were widely spread in Japan primarily via clinically normal carriers and identified via manifesting patients. Furthermore, genotype-phenotype analyses of patients reported in this study and the previous studies imply that clinical variability is ascribed to multiple factors including the size of duplications/triplications as a critical factor.

Keywords: *BHLHA9*, Split-hand/foot malformation, Long bone deficiency, Gollop-Wolfgang complex, Expressivity, Penetrance, Susceptibility, Japanese founder copy number gain

Introduction

Split-hand/foot malformation (SHFM), also known as ectrodactyly, is a rare limb malformation involving the central rays of the autopod [1,2]. It presents with median clefts of the hands and feet, aplasia/hypoplasia of the phalanges, metacarpals, and metatarsals, and syndactyly. SHFM results from failure to maintain the central portion of the apical ectodermal ridge (AER) in the developing autopod [1,2]. SHFM is divided into two forms: a non-syndromic form with limb-confined manifestations and a syndromic form with extra-limb manifestations [2]. Furthermore, non-syndromic SHFM can occur as an isolated abnormality confined to digits (hereafter, SHFM refers to this type) or in association with other limb abnormalities as observed in SHFM with long bone deficiency (SHFLD) usually affecting the tibia and in Gollop-Wolfgang complex (GWC) characterized by femoral bifurcation [1,2]. Both syndromic and non-syndromic forms are associated with wide expressivity and penetrance even among members of a single family and among limbs of a single patient [2].

SHFM and SHFLD are genetically heterogeneous conditions reviewed in ref. [2]. To date, SHFM has been identified in patients with heterozygous deletions or translocations involving the *DLX5–DLX6* locus at 7q21.2–21.3 (SHFM1) [3] (*DLX5* mutations have been detected recently), heterozygous duplications at 10q24 (SHFM3), heterozygous mutations of *TP63* at 3q27 (SHFM4), heterozygous deletions affecting *HOXD* cluster at 2q31 (SHFM5), and biallelic mutations of *WNT10B* at 12q31 (SHFM6); in addition, SHFM2 has been assigned to Xq26 by linkage analyses in a large Pakistani kindred [2]. Similarly, a genomewide linkage analysis in a large consanguineous family has identified two SHFLD susceptibility loci, one at 1q42.2–q43 (SHFLD1) and the other at 6q14.1 (SHFLD2); furthermore, after assignment of another SHFLD locus to 17p13.1–13.3 [4], duplications at 17p13.3 (SHFLD3) have been found in patients with SHFLD reviewed in ref. [2]. However, the GWC locus (loci) remains unknown at present.

The duplications at 17p13.3 identified to date are highly variable in size, and harbor *BHLHA9* as the sole gene within the smallest region of overlap [5-9]. *Bhlha9*/*bhlha9* is expressed in the limb bud mesenchyme underlying the AER in mouse and zebrafish embryos, and *bhlha9* knockdown has resulted in shortening of the pectoral fins in zebrafish [6]. Furthermore, *BHLHA9*-containing duplications have been identified not only in patients with SHFLD but also in those with SHFM and clinically normal family members [4-10]. These findings argue for a critical role of *BHLHA9* duplication in the development of SHFM and SHFLD, with variable expressivity and incomplete penetrance.

In this study, we report on *BHLHA9*-containing duplications/triplications with an identical fusion point and various haplotype patterns that were associated with a range of limb malformations including GWC, and discuss on characteristic clinical findings, genomic basis of Japanese founder copy number gains, and underlying factors for phenotypic variability.

Materials and methods

Patients/subjects

We studied 68 patients with SHFM (n = 55), SHFLD (n = 11), or GWC (n = 2), as well as 60 clinically normal relatives, from 51 Japanese families; the pedigrees of 27 of the 51 families and representative clinical findings are shown in Figure 1. All the probands 1–51 had a normal karyotype. Southern blot analysis for SHFM3 locus had been performed in 28 probands with SHFM, indicating 10q24 duplications in two of them [11]. Clinical features including photographs and roentgenograms of a proband with GWC and his brother with SHFLD (family 23 in Figure 1A) were as described previously [12]. The residencies of families 1–51 were widely distributed throughout Japan.

Ethical approval and samples

This study was approved by the Institutional Review Board Committees of Hamamatsu University School of

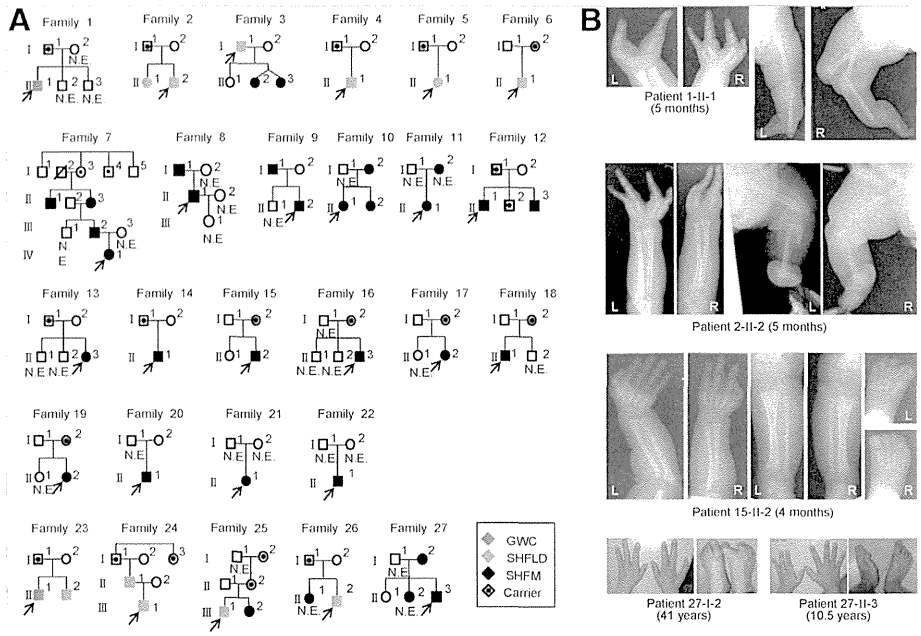

Figure 1 Clinical summary. A. Pedigrees of 27 Japanese families with duplications (families 1–22) and triplications (families 23–27) of a ~200 kb region involving *BHLHA9*. The duplications/triplications are associated with GWC, SHFLD, SHFM, or normal phenotype (carriers). N.E.: Not examined molecularly. **B.** Representative clinical findings. Each patient is indicated by a family-generation-individual style and corresponds to the patient/subject shown in Figure 1A and Additional file 5. The top panel: GWC with right bifid femur; the second panel: SHFLD with bilateral tibial deficiencies, the third panel: SHFM with polydactyly; and the bottom panel: SHFM.

Medicine, RIKEN, and National Center for Child Health and Development, and was performed using peripheral leukocyte samples after obtaining written informed consent for the molecular analysis and the publication of genetic and clinical data after removing information for personal identification (e.g., name, birthday, and facial photograph) from the adult subjects (^{3} 20 years) or from the parents of the child subjects (below 20 years). Furthermore, informed assent was also obtained from child subjects between 6–20 years.

Samples and primers

The primers utilized in this study are summarized in Additional file 1.

Molecular studies

Sanger sequencing, fluorescence *in situ* hybridization (FISH), microsatellite genotyping, Southern blotting, and bisulfite sequencing-based methylation analysis were performed by the standard methods, as reported previously [13]. Quantitative real-time PCR (qPCR) analysis was carried out by the SYBR Green methods on StepOnePlus system, using *RNaseP* as an internal control (Life Technologies). Genomewide oligonucleotide-based array comparative genomic hybridization (CGH) was performed with a catalog human array (4 × 180 K format, ID G4449A) according to the manufacturer's instructions (Agilent Technologies), and obtained copy number variants/polymorphisms were screened with Agilent Genomic Workbench software using the Database of Genomic Variants (http://dgv.tcag.ca/dgv/app/home). Sequencing of a long region encompassing *BHLHA9* was performed with the Nextera XT kit on MiSeq (Illumina), using SAMtools v0.1.17 software (http://samtools.sourceforge.net/). Exome sequencing was performed as described previously [14].

Assessment of genomic environments around the fusion points

Repeat elements around the fusion point were searched for using Repeatmasker (http://www.repeatmasker.org). Rearrangement-inducing DNA features were investigated for 300 bp regions at both the proximal and the distal sides of each breakpoint, using GEECEE (http://emboss.bioinformatics.nl/cgi-bin/emboss/geecee) for calculation of the average GC content, PALINDROME (http://mobyle.pasteur.fr/cgi-bin/portal.py#forms::palindrome) and Non-B DB (http://nonb.abcc.ncifcrf.gov) for the examination of the palindromes and non-B (non-canonical) structures, and Fuzznuc (http://emboss.bioinformatics.nl/cgi-bin/emboss/fuzznuc) for the assessment of rearrangement-associated sequence motifs and tri/tetranucleotides [15-20]. For controls, we examined 48 regions of 600 bp long selected at an interval of 1.5 Mb from the entire chromosome 17.

Statistical analysis

The statistical significance of the frequency was analyzed by the two-sided Fisher's exact probability test.

Results

Sequence analysis of the known causative/candidate genes

We performed direct sequencing for the previously known causative genes (*DLX5*, *TP63*, and *WNT10B*) reviewed in ref. [2] in the probands 1–51. Although no pathologic mutation was identified in *DLX5* and *TP63*, the previously reported homozygous missense mutation of *WNT10B* (c.944C > T, p.R332W) [21] was detected in the proband 48 with SHFM who was born to healthy consanguineous parents heterozygous for this mutation. In addition, while no variation was detected in *DLX5* and *WNT10B*, rs34201045 (4 bp insertion polymorphism) in *TP63* [21] was detected with an allele frequency of 61%.

We also examined *BHLHA9*, because gain-of-function mutations of *BHLHA9* as well as *BHLHA9*-harboring duplications may lead to limb malformations. No sequence variation was identified in the 51 probands.

Array CGH analysis

Array CGH analysis was performed for the probands 1–51, showing increased copy numbers at 17p13.3 encompassing *BHLHA9* (SHFLD3) in the probands 1–27 from families 1–27 (Figure 1A). Furthermore, heterozygous duplications at 10q24 (SHFM3) were detected in the probands 49–51, i.e., a hitherto unreported patient with paternally inherited SHFM (his father also had the duplication) and the two patients who had been indicated to have the duplications by Southern blot analysis [11]. No copy number alteration was observed at other SHFM/SHFLD loci in the probands 1–27 and 49–51. In the remaining probands 28–48, there was no copy number variation that was not registered in the Database of Genomic Variants.

Identical fusion points in *BHLHA9*-containing duplications/triplications

The array CGH indicated that the increased copy number regions at 17p13.3 were quite similar in the physical size in the probands 1–27 and present in three copies in the probands 1–22 and in four copies in the probands 23–27 (Figure 2A). Thus, FISH analysis was performed using 8,259 bp PCR products amplified from this region, showing two signals with a different intensity that was more obvious in the probands 23–27 (Figure 2A).

We next determined the fusion points of the duplications/triplications (Figure 2B). PCR products of 2,195 bp long were obtained with P1/P2 primers in the probands 1–27, and the fusion point was determined by direct sequencing for 418 bp PCR products obtained with P3/P4 primers. The fusion point was identical in all the probands 1–27; it resided on intron 1 of *ABR* and intron 1 of *YWHAE*, and was associated with a 4 bp microhomology.

Then, we performed qPCR analysis for a 214 bp region harboring the fusion point, using P5/P6 primers (Figure 2C and Additional file 2). The fusion point was present in a single copy in the probands 1–22 and in two copies in the probands 23–27. The results showed that the identical genomic segment harboring *BHLHA9* was tandemly duplicated in the probands 1–22 and triplicated in the probands 23–27. According to GRCh37/hg19 (http://genome.ucsc.edu/), the genomic segment was 210,050 bp long.

We also performed array CGH and qPCR for the fusion point in 15 patients other than the probands and 47 clinically normal relatives from the 27 families (Figures 1 and 2C). The duplications/triplications were identified in all the 15 patients. Thus, in a total of 42 patients, duplications/triplications were found in 29 SHFM patients, 11 SHFLD patients, and two GWC patients. Furthermore, the duplications/triplications were also present in 22 of the 47 clinically normal relatives. In particular, they were invariably identified in either of the clinically normal parents when both of them were examined; they were also present in other clinically normal relatives in families 7, 12, 24, and 25.

Since the above data indicated the presence of duplications/triplications in clinically normal subjects, we performed qPCR for the fusion point in 1,000 Japanese controls. The fusion point was detected in a single copy in two subjects (Subjects 1 and 2 in Figure 2C). We also performed array CGH in 200 of the 1,000 controls including the two subjects, confirming the duplications in the two subjects and lack of other copy number variations, including deletions involving *BHLHA9*, which were not registered in the Database of Genomic Variants in the 200 control subjects. The frequency of duplications/triplications was significantly higher in the probands than in the control subjects (27/51 vs. 2/1,000, $P = 3.5 \times 10^{-37}$).

Various haplotype patterns on the duplicated/triplicated segments

We carried out genotyping for rs3951819 (A/G SNP on *BHLHA9*) and *D17S1174* (CA repeat microsatellite locus) on the genomic segment subjected to duplications/triplications (Figure 2A), and determined rs3951819-*D17S1174* haplotype patterns. Representative results are shown in Figure 2D, and all the data are available on request. Various haplotype patterns were identified on the single, the duplicated, and the triplicated segments, and the [A-14] haplotype was most prevalent on the duplicated/triplicated segments (Table 1). While the distribution of CA repeat lengths on the single segments was discontinuous, similar discontinuous distribution was

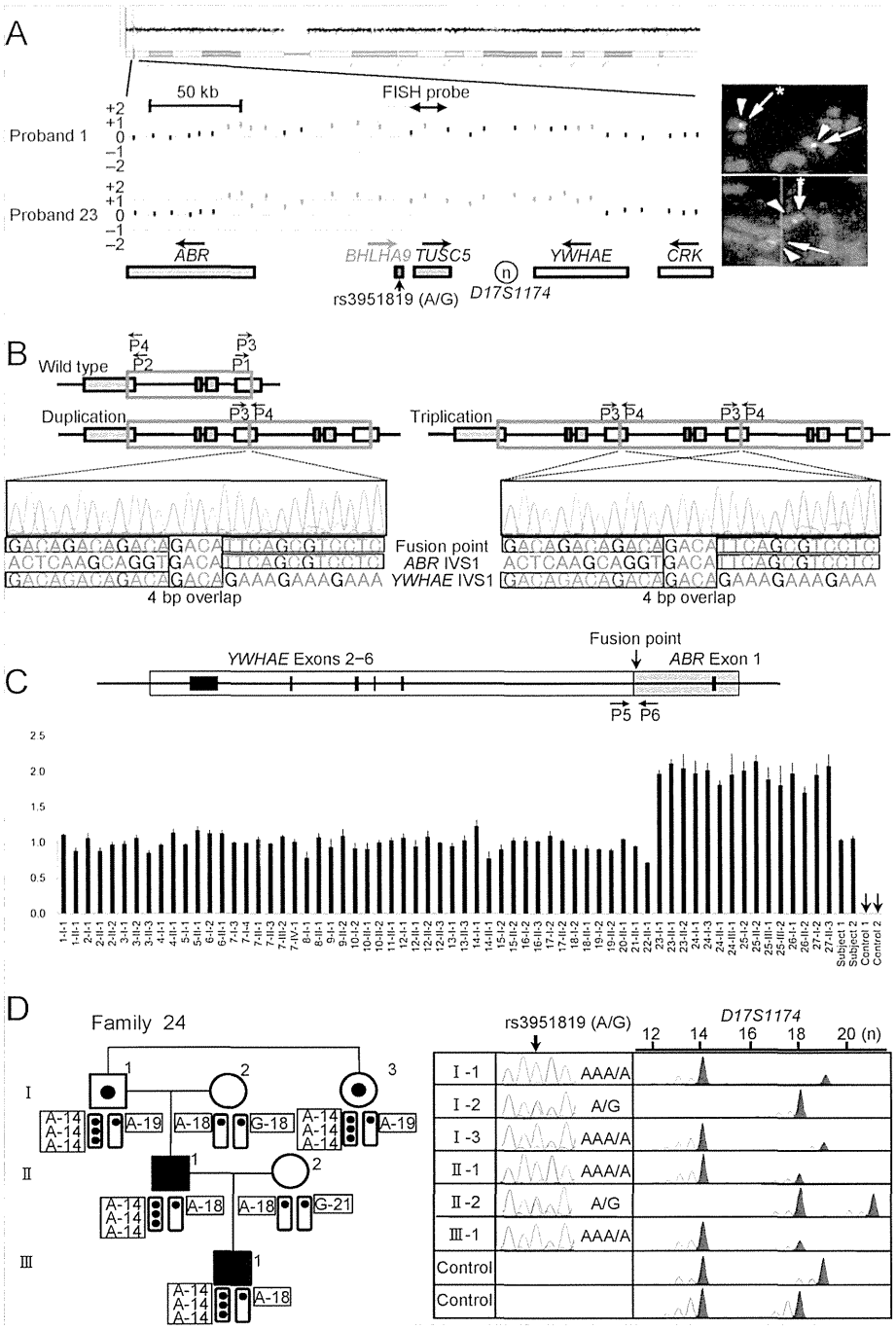

Figure 2 (See legend on next page.)

(See figure on previous page.)
Figure 2 Identification and characterization of the duplications/triplications involving *BHLHA9* at chromosome 17p13.3. A. Array CGH and FISH analyses in proband 1 and proband 23 with GWC. In array CGH analysis, the black and the red dots denote the normal and the increased copy numbers, respectively. Since the log2 signal ratios for a ~200 kb region encompassing *BHLHA9* are around +0.5 in the proband 1 and around +1.0 in the proband 23, this indicates the presence of three and four copies of this region in the two probands, respectively. In FISH analysis, two red signals with an apparently different density are detected by the 8,289 bp PCR probe (the stronger signals are indicated with asterisks). The green signals derive from an internal control probe (CEP17). The arrows on the genes show transcriptional directions. Rs3951819 (A/G) resides within *BHLHA9*. **B**. Determination of the fusion point. The fusion has occurred between intron 1 of *ABR* and intron 1 of *YWHAE*, and is associated with a 4 bp (GACA) microhomology. P1–P4 show the position of primers. **C**. Quantitative real-time PCR analysis. The upper part denotes the fusion point. P5 & P6 show the position of primers. The lower part shows the copy number of the fusion point in patients/subjects with duplications/triplications (indicated by a family-generation-individual style corresponding to that in Figure 1 and Additional file 5). Subject-1 and subject-2 denote the two control subjects with the duplication, and control-1 and control-2 represent normal subjects without the duplication/triplication. **D**. The rs3951819 (A/G SNP)–*D17S1174* (CA repeat number) haplotype patterns in family 24. Assuming no recombination between rs3951819 and *D17S1174*, the haplotype patterns of the family members are determined as shown here. The haplotype patterns of the remaining families have been interpreted similarly.

also observed in the Japanese general population (see Additional file 3).

Genomic environments around the breakpoints

The breakpoint on *YWHAE* intron 1 resided on a simple *Alu* repeat sequence, and that on *ABR* intron 1 was present on a non-repetitive sequence. There was no low copy repeat around the breakpoints. Comparison of the frequencies of known rearrangement-inducing DNA features between 600 bp sequences around the breakpoints and those of 48 regions selected at an interval of 1.5 Mb from chromosome 17 revealed that palindromes, several types of non-B DNA structures, and a rearrangement-associated sequence motif were abundant around the breakpoint on *YWHAE* intron 1 (see Additional file 4).

Clinical findings of families 1–27

Clinical assessment revealed several notable findings. First, duplications/triplications were associated with SHFM, SHFLD, GWC, or normal phenotype, with inter- and intra-familial clinical variability (Figure 1A). Second, in the 42 patients, split hand (SH) was more prevalent than split foot (SF) (41/42 vs. 17/42, $P = 6.2 \times 10^{-9}$), and long bone defect (LBD) was confined to lower extremities (0/42 vs. 13/42, $P = 4.1 \times 10^{-5}$) (Table 2 and Additional file 5). Third, there was no significant sex difference in the ratio between patients with limb malformations and patients/carriers with duplications/triplications (26/38 in males vs. 16/26 in females, $P = 0.60$) (Table 2 and Additional file 5). Fourth, the ratio of LBD positive families was significantly higher in triplications than in duplications (4/5 vs. 16/22, $P = 0.047$) (Figure 1A and Table 2). Fifth, while the duplications/triplications were transmitted from patients to patients, from carriers to patients, and from a carrier to a carrier (from I-1 to II-2 in family 12), transmission from a patient to a carrier was not identified (Figure 1A); it should be pointed out, however, that molecular analysis in a clinically normal child born to an affected parent was possible only in a single adult subject (II-1 in family 27), and that molecular analysis in clinically

Table 1 The rs3951819 (A/G SNP) – *D17S1174* (CA repeat number) haplotype

Patterns of the 210,050 bp segment subjected to copy number gains	
Haplotype pattern	**Family**
<Single segment>	
[A-14]	1, 5, 9, 15, 17, 19, 23, 26
[A-16]	12
[A-18]	3, 14, 15, 24, 25, 26
[A-19]	2, 6, 13, 19, 20, 24, 25, 27
[A-21]	5, 23
[G-12]	17
[G-14]	2, 3, 6, 12, 13, 19, 26
[G-18]	3, 5, 17, 18, 24, 25
[G-19]	9, 12, 18, 20, 25
[G-21]	1, 9, 19, 24, 27
[A-14] or [G-14]	16
[A-18] or [G-18]	4
[A-19] or [G-19]	4
[A-21] or [G-21]	16
<Duplicated segments>	
[A-14] + [A-14]	5, 12, 13, 14, 15, 20
[A-14] + [A-18]	1
[A-14] + [G-18] or [G-14] + [A-18]	2, 3, 4, 6, 9, 16, 17
[A-14] + [G-18] or [A-14] + [G-19]	18
[A-14] + [G-14] or [G-14] + [G-14]	19
<Triplicated segments>	
[A-14] + [A-14] + [A-14]	23, 24
[A-14] + [A-14] + [G-14]	25
[A-14] + [A-19] + [A-19]	26
[A-14] + [G-18] + [G-18] or [G-14] + [A-18] + [G-18]	27

The haplotype patterns written in the left column have been detected in at least one patient/subject in the families described in the right column.
Genotyping could not be performed in several patients/subjects who had been repeatedly examined previously, because of the extremely small amount of DNA samples that were virtually used up in the sequencing and array CGH analyses.

Table 2 Summary of clinical findings in patients/carriers with duplications/triplications involving *BHLHA9*

	SHFM (+) patients			LBD (+) patients			Patient ratio*			LBD (+) families		
	SH	SF	*P*-value	U-LBD	L-LBD	*P*-value	Male	Female	*P*-value	Trip	Dup	*P*-value
This study	41/42	17/42	6.2×10^{-9}	0/42	13/42	4.1×10^{-5}	26/38	16/26	0.60	4/5	16/22	0.047
Previous studies	63/84	23/84	8.6×10^{-10}	11/91	42/91	5.7×10^{-7}	68/114	31/79	5.7×10^{-3}	...	...	...
Sum	104/126	40/126	1.1×10^{-16}	11/133	55/133	3.0×10^{-10}	94/152	47/105	7.6×10^{-3}	...	...	...

SHFM: split-hand/foot malformation; SH: split hand; SF: split foot; LBD: long bone deficiency; U: upper; L: lower; Trip: triplication; and Dup: duplication.
In the previous studies, patients without detailed phenotypic description and those of unknown sex have been excluded (3–9).
*The ratio between patients with limb malformations and patients/carriers with duplications/triplications, i.e. the number of patients over the number of patients plus carriers.

normal children <20 years old was possible only in two subjects (II-2 in family 12 and II-1 in family 15). Lastly, limb malformation was inherited in an apparently autosomal dominant manner (from patients to patients), or took place as an apparently *de novo* event or as an apparently autosomal recessive trait (from clinically normal parents to a single or two affected children) (Figure 1A).

Attempts to identify a possible modifier(s)

The variable expressivity and incomplete penetrance in families 1–27 suggest the presence of a possible modifier (s) for the development of limb malformations. Thus, we performed further molecular studies in patients/subjects in whom DNA samples were still available, and compared the molecular data between patients with SHFM and those with SHFLD for the assessment of variable expressivity and between SHFM, SHFLD, or total patients and carriers for the evaluation of incomplete penetrance.

We first examined the possibility that the modifier(s) resides within or around *BHLHA9* (see Additional file 6). There was no *BHLHA9* mutation in all the 21 examined probands with SHFM, SHFLD, or GWC, as described in the section of "Sequence analysis of the known causative/candidate genes". The rs3951819 A/G SNP pattern on the duplicated/triplicated segments was apparently identical between patients and carriers (e.g. Figure 2D), and the frequency of A/G allele on the normal chromosome 17 was similar between SHFM and SHFLD patients and between SHFM, SHFLD, or total patients and carriers (see Additional file 7). The results of other known SNPs on *BHLHA9* (rs185242872, rs18936498, and rs140504068) were not informative, because of absence or extreme rarity of minor alleles. Furthermore, in SHFM families 7, 12, and 18, sequencing of a 7,406 bp region encompassing *BHLHA9* and Southern blot analysis using five probes and *Mfe*I-, *Ssp*I-, and *Sac*I-digested genomic DNA revealed no variation specific to the patients, and methylation analysis for a CpG rich region at the upstream of *BHLHA9* delineated massive hypomethylation in all the patients/carriers examined.

Next, we examined the possibility that a variant(s) of known causative genes constitutes the modifier(s). Since rs34201045 in *TP63* was identified in the mutation analysis, we compared rs34201045 genotyping data between the 27 probands and the 15 carriers. The allele and genotype frequencies were similar between SHFM and SHFLD patients and between SHFM, SHFLD, or total patients and carriers (see Additional file 8).

We finally performed exome sequencing in SHFM families 13 and 17–19. However, there was no variation specific to the patients. In addition, re-examination of the genomewide array CGH data showed no discernible copy number variation specific to the patients.

Discussion

BHLHA9 overdosage and clinical characteristics

We identified duplications/triplications of a ~ 200 kb genomic segment involving *BHLHA9* at 17p13.3 in 27 of 51 families with SHFM, SHFLD, or GWC. To our knowledge, this is the first study revealing the underlying genetic factor for the development of GWC, and demonstrating the presence of triplications involving *BHLHA9* that were suggested but not confirmed in the previous studies [5,9]. Furthermore, this study indicates that *BHLHA9*-containing duplications/triplications are the most frequent underlying factor for the development of limb malformations at least in Japan. Notably, SHFLD and GWC with LBD were significantly more frequent in patients with triplications than in those with duplications, and the duplications/triplications were identified in clinically normal familial members and in the general population. These findings imply that increased *BHLHA9* copy number constitutes a strong susceptibility, rather than a causative, factor with a dosage effect for the development of a range of limb malformations. Since *Bhlha9* is expressed in the developing ectoderm adjacent to the AER rather than the AER itself in mouse embryos [6], *BHLHA9* appears to play a critical role in the limb development by interacting with the AER. While the duplications/triplications identified in this study included *TUSC5* and generated an *ABR-YWHAE* chimeric gene (Figure 2C), *TUSC5* duplication and the chimeric gene formation are not common findings in the previously reported patients with duplications at 17p13.3 and SHFM and/or SHFLD [5-9]. In addition, none of *Tusc5*, *Abr*, and *Ywhae* is specifically expressed in the developing mouse limb buds [22] (A Transcriptome Atlas Database

for Mouse Embryo of Eurexpress Project, http://www.eurexpress.org/ee/project/).

Several clinical findings are noteworthy in patients/subjects with duplications/triplications. First, SH was more frequent than SF in this study as well as in the previous studies, and LBD was confined to lower extremities in this study and was more frequent in lower extremities than in upper extremities in the previous studies (Table 2) [4-10]. This implies that *BHLHA9* overdosage exerts differential effects on the different parts of limbs. Second, while limb malformations were similarly identified between males and females in this study, they were more frequently observed in males than in females in the previous studies (Table 2) [4-10]. In this regard, it has been reported that testosterone influences the digital growth pattern as indicated by the lower second to fourth digit length ratio in males than in females [23-25], and that Caucasian males have higher serum testosterone values and lower second to fourth digit length ratios than Oriental males [26,27]. Such testosterone effects on the digital growth pattern with ethnic difference may explain why male dominant manifestation was observed in the previous studies primarily from Caucasian countries and was not found in this study. Lastly, LBD was more prevalent in patients with triplications than in those with duplications. This suggests that LBD primarily occurs when the effects of *BHLHA9* overdosage are considerably elevated.

Genomic basis of the Japanese founder copy number gains

The duplications/triplications were associated with the same fusion point and variable haplotype patterns. Since there was no sequence homology or low-copy repeats around the breakpoints, it is unlikely that such duplications/triplications were recurrently produced in different individuals by non-allelic homologous recombination (NAHR) [17,20]. Instead, it is assumed that a Japanese founder duplication took place in a single ancestor, and was spread with subsequent triplication and modification of the haplotype patterns.

The most likely genomic basis of the Japanese duplications/triplications is illustrated in Additional file 9. Notably, a 4 bp (GACA) microhomology was identified at the duplication fusion point (Figure 2B). A microhomology refers to two to five nucleotides common to the sequences of the two breakpoints, and is found as an overlapping sequence at the join point [16,19,20]. This suggests that the Japanese founder duplication was generated by replication-based mechanisms such as fork stalling and template switching (FoSTeS) and microhomology-mediated break-induced replication (MMBIR), because the presence of such a microhomology is characteristic of FoSTeS/MMBIR [17-20]. Indeed, such a simple tandem duplication with a microhomology can be produced by one time FoSTeS/MMBIR [17-20], although it could also be generated by non-homologous end-joining (NHEJ) [17]. Since the [A-14] haplotype was most prevalent on the duplicated/triplicated segments, it is inferred that a genomic rearrangement occurred in an ancestor with the [A-14] haplotype, yielding the founder duplication with the [A-14] + [A-14] haplotype. Furthermore, the presence of multiple stimulants for genomic rearrangements around the breakpoint on *YWHAE* intron 1 would have facilitated the generation of the founder duplication. In particular, non-B structures are known to stimulate the occurrence of both replication-based FoSTeS/MMBIR and double-strand breaks and resultant NHEJ [17,28,29], although the relative importance of each non-B DNA structure is largely unknown.

Subsequent triplication and haplotype modification can develop from the Japanese founder duplication through unequal interchromatid and interchromosomal recombinations [17,20]. Indeed, a tandem triplication with the [A-14] + [A-14] + [A-14] haplotype can be generated by unequal exchange between sister chromatids with the [A-14] + [A-14] haplotype, and various haplotype patterns are yielded by unequal interchromosomal exchanges involving the duplicated or triplicated segments. Furthermore, the haplotype variation would be facilitated by unequal exchanges between sister chromatids harboring duplications/triplications with various haplotype patterns and by the further unequal interchromosomal exchanges.

Underlying factors for the phenotypic variability

The duplications/triplications were accompanied by limb malformations with variable expressivity and incomplete penetrance. Although this may suggest the presence of a possible modifier(s) for the development of limb malformations, such a modifier(s) was not detected. In particular, while patient-to-carrier transmission of duplications/triplications was not identified in this study, even patient-to-carrier-to-patient transmission has been reported in three pedigrees [5,6,10]. Such transmission pattern with incomplete penetrance characterized by skipping of a generation is apparently inexplicable by assuming a modifier (s) interacting with *BHLHA9* or independent of *BHLHA9* on the duplication/triplication positive chromosome 17, on the normal chromosome 17, or on other chromosomes (Figure 3, Models A, B, and C, see also the legends in Figure 3).

In this regard, it is noteworthy that the development of limb malformations is obviously dependent on the size of genomic segment subjected to copy number gains. Actually, limb malformation has occurred in only one of 21 large duplications encompassing *BHLHA9* (average 1.55 Mb, mean 1.12 Mb) and in 29 of 80 small duplications encompassing *BHLHA9* (average 244 kb, mean 263 kb) ($P = 5.9 \times 10^{-3}$) [8]. Consistent with this, the patients with large and

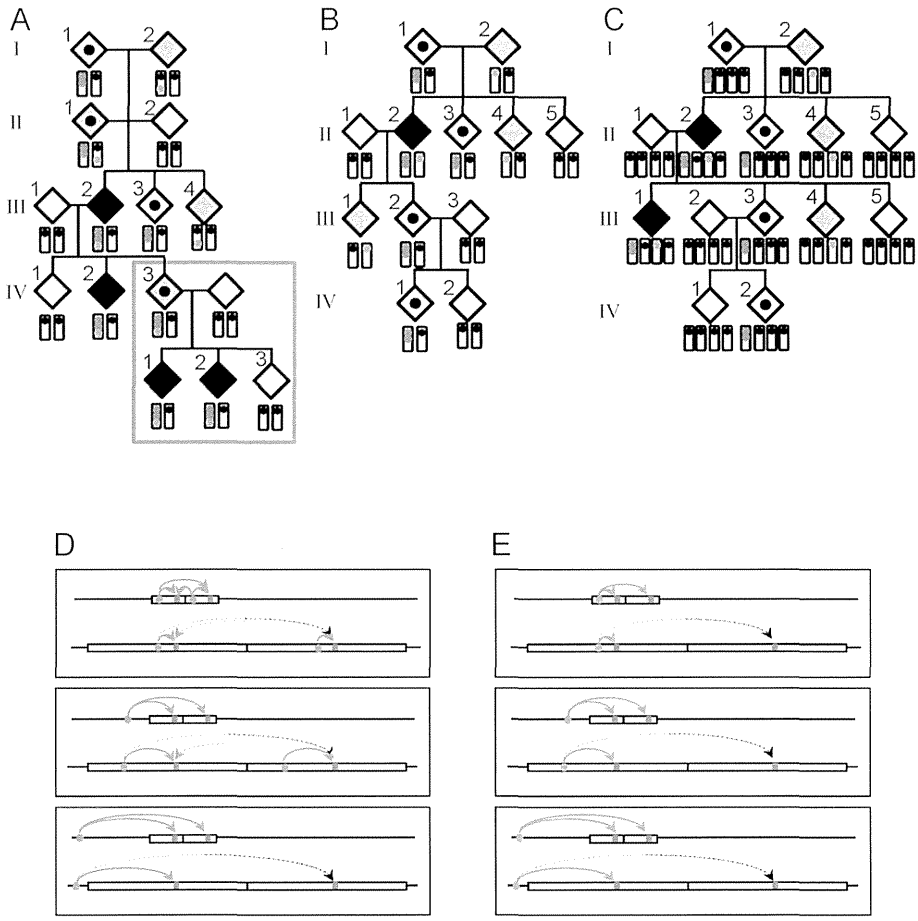

Figure 3 Models for a modifier(s) and effects of the duplication size. In models **A–C**, the yellow bars show chromosome 17, and the light green bars indicate other chromosomes. The two red dots represent the duplication at 17p13.3, and the blue dots indicate a putative modifier(s). Black painted diamonds represent limb malformation positive patients, dot-associated and gray painted diamonds indicate clinically normal carriers with the duplications and the modifier(s) respectively, and white painted diamonds denote clinically normal subjects without both the duplications and the modifier(s). **A**. This model assumes that co-existence of the duplication and a *cis*-acting modifier(s) causes limb malformation. If co-existence of the duplication and the *cis*-acting modifier(s) is associated with incomplete penetrance, this can explain all the transmission patterns observed to date, including the patient-to-carrier transmission and the presence of ≥ 2 affected children. **B**. This model postulates that the presence of a *cis*-acting modifier(s) on the normal chromosome 17 leads to limb malformation by enhancing the expression of the single *BHLHA9*, together with duplicated *BHLHA9* on the homologous chromosome. **C**. This model postulates that co-existence of the duplication at 17p13.3 and a modifier(s) on other chromosome causes limb malformation. In models **D–E**, the red bars represent *BHLHA9*, the blue circles indicate a physiological cis-regulatory element for *BHLHA9*, and the green circles indicate a non-physiological modifier(s) for *BHLHA9*. **D**. The physiological cis-regulatory element may be duplicated or non-duplicated, depending on its position relative to the size of the duplications. *BHLHA9* expression can be higher in small duplications than large duplications. **E**. The non-physiological modifier(s) can be transferred to various positions of the duplication positive chromosome 17, depending on the recombination places (see Model A). *BHLHA9* expression can be higher in small duplications than large duplications irrespective of the position of the modifier(s).

small duplications were ascertained primarily due to developmental retardation and limb malformation, respectively [8]. It is likely that a physiological cis-regulatory element for *BHLHA9* (e.g., an enhancer) can frequently but not invariably work on both of the duplicated *BHLHA9* when the duplication size is small but is usually incapable of working on duplicated *BHLHA9* when the duplication size is large, probably because of the difference in the chromatin structure (see Model D in Figure 3). Similar findings have also been reported in other genes. For example, small (~150 kb) and relatively small (600–800 kb) duplications involving a putative testis-specific enhancer(s) for *SOX9* have caused 46,XX testicular and ovotesticular disorders of sex development respectively, whereas large duplications (~2 Mb) involving the enhancer(s) have permitted normal ovarian development in 46,XX individuals [30].

Thus, a plausible explanation may be that a range of limb malformations emerge when the effects of *BHLHA9* overdosage exceed the threshold for the development of SHFM, SHFLD, or GWC, depending on the conditions of